

Measurement of local entrainment rate in the initial region of axisymmetric turbulent air jets

By B. J. HILL

Mechanical Engineering Department, Imperial College, London

(Received 11 June 1971)

The local entrainment rate in the initial region of axisymmetric turbulent air jets has been measured by a novel method, which is an adaptation of the 'porous-wall' technique used by Ricou & Spalding (1961). The local entrainment rate, which is independent of the nozzle Reynolds number for values greater than 6×10^4 , is strongly dependent upon the axial distance. At an axial distance of one nozzle diameter the local entrainment rate is only about one-third of that in the fully developed jet; the entrainment rate increases with increasing axial distance to reach the fully developed value at an axial distance of about thirteen nozzle diameters.

1. Introduction

Fluid jets have the characteristic of entraining, i.e. drawing in, the surrounding fluid so that the mass flow rate of the jet increases with axial distance from the jet origin. The property under consideration here is the mass flow rate in the jet, m , and in particular the rate of change of mass flow rate dm/dx , which is equal to the local entrainment rate dm_e/dx . For an axisymmetric jet

$$m = 2\pi \int_0^\infty \bar{\rho u} r dr, \quad (1)$$

where ρ is the fluid density, u is the fluid velocity in the axial direction x and r is the radial distance.

The law governing the entrainment in axisymmetric free jets is well established experimentally for the region of fully developed flow, i.e. for axial distance greater than about fifteen nozzle diameters. For the initial region of developing flow the experimental data are not very reliable but most investigators have concluded that the local entrainment rate is lower than that in the fully developed flow.

1.1. *The region of fully developed flow*

In fully developed axisymmetric free jets the mass flow rate of the jet is observed to increase linearly with axial distance according to the relation

$$\frac{1}{M^{\frac{1}{2}} \rho_s^{\frac{1}{2}}} \frac{dm}{dx} = C_1, \quad (2)$$

where M is the momentum flux of the jet, ρ_s is the density of the surrounding fluid and C_1 is a constant; this result holds irrespective of the density ratio ρ_0/ρ_s

(Ricou & Spalding 1961), ρ_0 being the fluid density at the nozzle. If the velocity and density of the fluid are uniform across the jet nozzle an alternative form of (2) is

$$\frac{D}{m_0} \left(\frac{\rho_0}{\rho_s} \right)^{\frac{1}{2}} \frac{dm}{dx} = C_2, \quad (3)$$

where m_0 is the mass flow rate of the jet at the nozzle and D is the diameter of the nozzle. The constants C_1 and C_2 are related by $C_2 = 2C_1/\sqrt{\pi}$. The most reliable estimates of C_1 and C_2 , $C_1 = 0.28$ and $C_2 = 0.32$, come from the experiments of Ricou & Spalding.

Several different methods have been used to establish the value of C_2 in (3). Voorheis & Howe (1939), Albertson *et al.* (1948), Grimmer (1948) and Polomik (1948), for example, have calculated the changing mass flow rate in a jet by integration of velocity profiles obtained at different axial stations. The principal difficulty with this method is in the measurement of the low velocities near the jet edge, particularly at large axial distances; in practice this method is limited to axial distances less than about 60 nozzle diameters. In the experiments of Donald & Singer (1959) the liquid-into-liquid jet was directed into a concentric tube positioned downstream of the nozzle so that the jet just filled the entrance to the tube; the mass flow rate in the tube was presumed equal to the flow rate of the jet at the entrance to the tube. Although this method avoided the difficulties of measuring the velocity profile, the results were not reliable because, as was shown by flow visualization, it was not possible to avoid inflow of the surrounding fluid into the entrance of the tube.

Ricou & Spalding focused attention on the *entrained* flow instead of the *jet* flow. The jet was surrounded by a concentric chamber, closed at one end except for the jet nozzle and open at the other end to the atmosphere. The chamber was double-walled with a porous inner wall through which the measured entrainment air was supplied to the jet. When the pressure inside the chamber, but remote from the jet, was equal to the atmospheric pressure the rate of entrainment-air supply was presumed equal to that which would occur naturally in the absence of the chamber. The reliability of the porous-wall technique is shown by the constancy of the values of C_2 measured over a wide range of density ratio ρ_s/ρ_0 and axial distance x/D .

1.2. *The initial region of developing flow*

Voorheis & Howe, Albertson *et al.*, Grimmer and Polomik each made measurements of velocity profiles and calculated jet mass flow rates in the region immediately downstream of the nozzle, that is, in the region over which the velocity profile changes from that of the entering jet to that of fully developed flow. There were quantitative differences between their results but each of these investigators showed that the jet mass flow rate increased nonlinearly in this initial region, the entrainment rate being lower than in the fully developed jet. These results were confirmed qualitatively by Ricou's (1959) experiments in the range $2.5 \leq x/D \leq 7.5$. Donald & Singer, however, reported that the entrainment rate in the region $x/D < 14$ was not significantly different from that in the region of fully developed flow.

Because the methods considered so far measure the mass flow rate of the jet, in one way or another, they will be unsatisfactory for determining the local entrainment rate dm_e/dx where this varies with axial distance. For the local entrainment rate can only be deduced from the measurements of mass flow rate in the jet by numerical differentiation, a procedure in which much accuracy is lost. If, however, local entrainment can be measured directly, these indirect procedures are avoided. The following sections describe an adaptation of the porous-wall method which yields direct measurements of the local entrainment rate.

2. Apparatus

The method used was the same as the porous-wall technique of Ricou & Spalding except that the jet was directed through a short chamber open to the atmosphere at both ends. The chamber, which could be moved axially, was short enough for the measured rate of entrainment to correspond to the local entrainment rate at the mid-plane of the chamber.

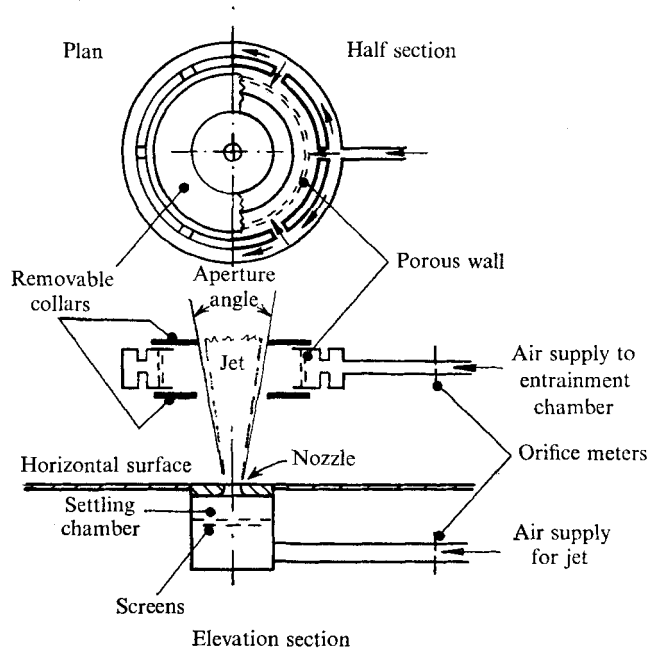


FIGURE 1. Arrangement of apparatus, not to scale. Nominal sizes: diameter of porous wall, 18 in.; axial length of chamber, $\frac{3}{4}$ in.; nozzle diameters, $\frac{3}{4}$, 1, $1\frac{1}{4}$, $1\frac{3}{4}$, $2\frac{1}{4}$ in.; horizontal surface 3 ft 6 in. square.

The apparatus is shown schematically in figure 1. The convergent jet nozzles, designed according to B.S. 1042, formed the outlet of a settling chamber which was fitted with screens to ensure uniform flow. The nozzle outlet was arranged flush with, and central to, a large horizontal surface. The entrainment chamber, which was concentric with the nozzle, could be moved vertically along its support

rods. The entrainment air was supplied to the chamber through six equally spaced inlets and the chamber was fitted with internal baffles to ensure a uniform distribution of air at the porous wall, which was made of porous polythene. Thin removable collars could be fixed to the top and bottom of the chamber in order to vary the effective chamber aperture. The gauge pressure within the chamber was measured on an electric micromanometer capable of detecting differences of 0.0001 in. watergauge. The flow rates of the air supply to the nozzle and the entrainment chamber were measured on orifice meters designed according to B.S. 1042.

3. Experimental results

3.1. Preliminary measurements in the region of fully developed flow

The technique was proved by making measurements in the region of fully developed flow, $14 \leq x/D \leq 58$. The results of Ricou & Spalding were reproduced successfully. The entrainment rate was found to be independent of the aperture angle† for angles greater than 30° and independent of the nozzle Reynolds number ($\equiv 4m_0/\pi D\mu$) for values greater than 3×10^4 ; the value of 0.32 for entrainment coefficient C_2 was confirmed.

The local entrainment rate dm_e/dx was identified with $\delta m_e/\delta x$, where δm_e is the mass flow rate through the porous wall which gives atmospheric pressure in the chamber and δx is the length of the chamber. From (3)

$$C_2 = \frac{D}{m_0} \left(\frac{\rho_0}{\rho_s} \right)^{\frac{1}{2}} \frac{dm_e}{dx} = \frac{D}{m_0} \left(\frac{\rho_0}{\rho_s} \right)^{\frac{1}{2}} \frac{\delta m_e}{\delta x}.$$

The density of the nozzle fluid, ρ_0 , was calculated from the pressure and temperature in the settling chamber on the assumption of reversible adiabatic flow through the nozzle. The difference in density between the nozzle fluid and the ambient air was always negligible except for the smallest nozzles for which the nozzle velocities were highest; the density ratio never fell outside the range $1.00 \leq \rho_0/\rho_s \leq 1.03$.

x/D	13.6	14.8	17.0	19.4	22.0
C_2	0.33	0.32	0.29	0.33	0.31
x/D	28.4	28.6	32.4	47.0	58.2
C_2	0.34	0.33	0.32	0.30	0.35

TABLE 1. Values of coefficient C_2 measured in the region of fully developed flow

3.2. Measurements in the initial region

The first series of experiments was designed to test the effect of the aperture angle on the measured entrainment rate. Figure 2 shows a typical result. For aperture angles of 30° or greater the entrainment mass flow rate $\delta m_e/m_0$ corre-

† The aperture angle is the angle at the apex of the cone formed between the nozzle outlet and the upper aperture of the entrainment chamber, i.e. the removable collar furthest from the nozzle.

sponding to atmospheric pressure within the chamber was independent of the aperture angle. For aperture angles less than 30° the chamber interfered with the jet flow and the apparent entrainment rate was markedly reduced. The smaller the aperture angle, the more steeply did the chamber pressure rise with increasing flow rate through the wall, and the more sensitive was the determination of the entrainment flow rate, which gave atmospheric pressure within the chamber. In order to obtain the maximum sensitivity whilst avoiding interference with the jet, the aperture angle was fixed at 30° for all later tests.

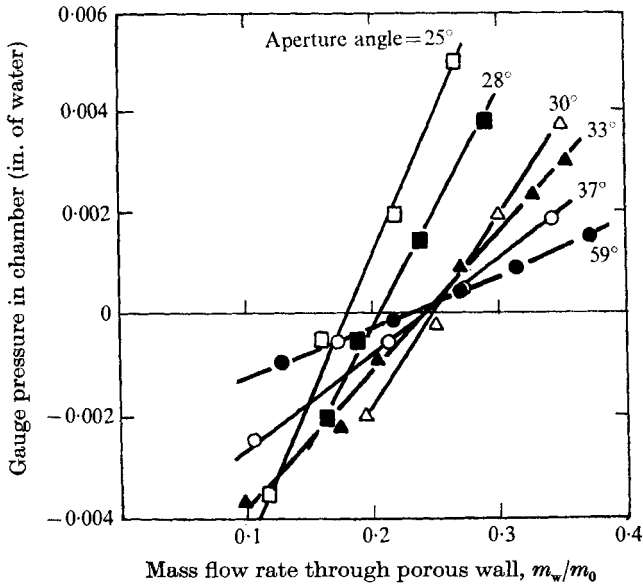


FIGURE 2. Variation of chamber pressure with flow rate through the porous wall for various apertures. Nozzle diameter 1 in., $x/D = 7.4$, $m_0 = 0.042$ lb/s.

The influence of the nozzle Reynolds number on the entrainment coefficient C_2 was investigated at various values of x/D spanning the initial region. The results, given in figure 3, show that the coefficient was independent of Reynolds number in the range covered by the experiments, $6-29 \times 10^4$, but that the coefficient was strongly dependent upon the axial distance. Mean values of the coefficient C_2 taken from figure 3 are plotted against axial distance x/D in figure 4. This graph shows that the coefficient C_2 reached the fully developed value at about $x/D = 13$.

The results displayed in figure 4 cannot be compared directly with other experimental data because none are available. Comparison can be made, however, between the measurements of mass flow rate derived from measurements of velocity profiles by various investigators and a curve of total entrained mass flow deduced from figure 4 by numerical integration. This comparison is displayed in figure 5 and shows that there is fair agreement for $x/D < 9$, but for greater axial distances the entrainment calculated from the measured velocity profiles is substantially less than that determined in the present investigation.

This discrepancy is consistent with the low values of C_2 for fully developed flow, which are obtained from these measured velocity profiles. Polomik, for example, using his own measurements together with those of Grimmer and of Taylor, deduces a value of $C_2 = 0.23$ for fully developed flow.

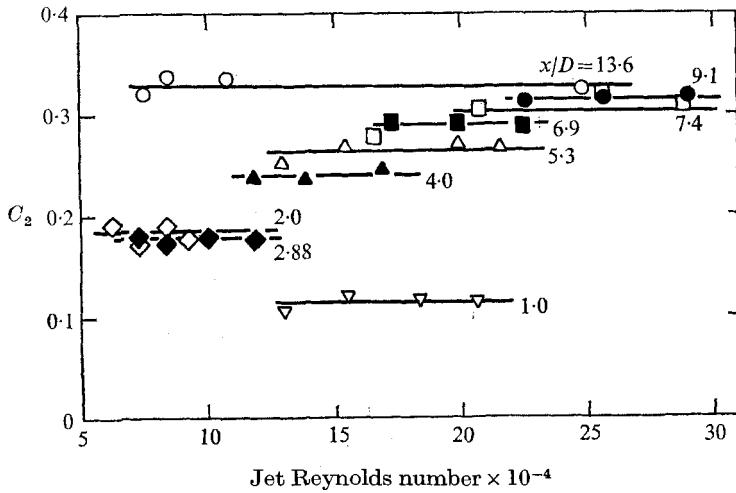


FIGURE 3. Variation of entrainment coefficient C_2 with Reynolds number in the initial region $\left(C_2 = \frac{D}{m_8} \left(\frac{\rho_0}{\rho_s}\right)^{\frac{1}{2}} \frac{\delta m_e}{\delta x}\right)$.

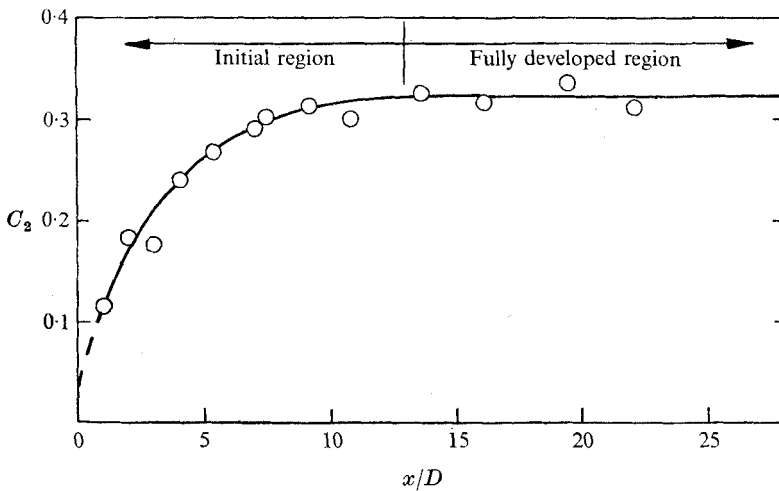


FIGURE 4. Variation of entrainment coefficient with axial distance.

4. Conclusions

(a) A method of measuring the local entrainment rate in axisymmetric free jets has been developed and validated by reproducing the well-established results for fully developed jet flow.

(b) Within the initial region, $0 \leq x/D \leq 13$, the entrainment coefficient C_2 varies with axial distance according to the curve of figure 4.

(c) The curve of figure 5, based on the measurements of local entrainment rate, represents the variation of total entrainment in the region of developing flow.

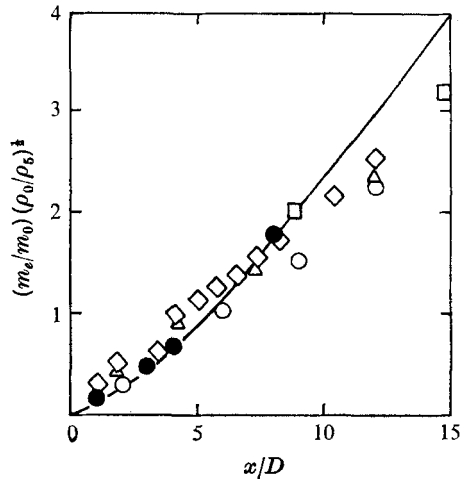


FIGURE 5. Variation of entrained mass flow rate with axial distance in the initial region. Experimental results: ●, Albertson *et al.*; △, Grimmert; ○, Polomik; ◇, Taylor; □, Voorheis & Howe; —, present investigation, deduced from figure 4.

REFERENCES

- ALBERTSON, M. L., DAI, Y. B., JENSEN, R. A. & HUNTER ROUSE, M. 1948 *Proc. A.S.C.E.* **74**, 10.
DONALD, M. B. & SINGER, H. 1959 *Trans. Inst. Chem. Engrs.* **37**, 255.
GRIMMETT, H. L. 1948 MS thesis, University of Illinois.
POLOMIK, E. E. 1948 MS thesis, University of Illinois.
RICOU, F. P. 1959 PhD thesis, University of London.
RICOU, F. P. & SPALDING, D. B. 1961 *J. Fluid Mech.* **11**, 21.
TAYLOR, J. F. 1948 MS thesis, University of Illinois.
VOORHEIS, T. S. & HOWE, E. D. 1939 *Proc. Pac. Coast Gas Ass.* **30**, 198.